ESC European Society of Cardiology

European Heart Journal (2021) **42**, 2935–2951
doi:10.1093/eurheartj/ehab316

TRANSLATIONAL RESEARCH
Valvular heart disease

DUSP26 induces aortic valve calcification by antagonizing MDM2-mediated ubiquitination of DPP4 in human valvular interstitial cells

Yongjun Wang[1†], Dong Han[2†], Tingwen Zhou[1†], Cheng Chen[3], Hong Cao[1], Joe Z. Zhang [4], Ning Ma[5], Chun Liu[4], Moshi Song[6], Jiawei Shi[1], Xin Jin [7]*, Feng Cao [2]*, and Nianguo Dong[1]*

[1]Department of Cardiovascular Surgery, Union Hospital, Tongji Medical College, Huazhong University of Science and Technology, 1277# Jiefang Avenue, Wuhan, Hubei 430022, China; [2]National Clinical Research Center for Geriatric Diseases, 2nd Medical Center, Chinese PLA General Hospital, 28# Fuxing Road, Beijing 100853, China; [3]Institute of Geriatrics, National Clinical Research Center for Geriatrics Disease, Chinese PLA General Hospital, 28# Fuxing Road, Beijing 100853, China; [4]Stanford Cardiovascular Institute, Stanford School of Medicine, 265 Campus Drive, Stanford, CA 94305, USA; [5]Bioland Laboratory (Guangzhou Regenerative Medicine and Health Guangdong Laboratory), 96# Xingdao South Road, Haizhu District, Guangzhou, Guangdong 510320, China; [6]Institute of Stem Cell and Regeneration, Chinese Academy of Sciences, 1# Beichen West Road, Beijing 100101, China; and [7]Department of Urology, The Second Xiangya Hospital, Central South University, 139# Renmin middle road, Changsha, Hunan 410011, China

Received 22 December 2020; revised 21 March 2021; editorial decision 30 April 2021; accepted 7 May 2021; online publish-ahead-of-print 28 June 2021

See page 2948 for the editorial comment on this article (doi: 10.1093/eurheartj/ehab381)

Aims The morbidity and mortality rates of calcific aortic valve disease (CAVD) remain high while treatment options are limited. Here, we evaluated the role and therapeutic value of dual-specificity phosphatase 26 (DUSP26) in CAVD.

Methods and results Microarray profiling of human calcific aortic valves and normal controls demonstrated that DUSP26 was significantly up-regulated in calcific aortic valves. ApoE$^{-/-}$ mice fed a normal diet or a high cholesterol diet (HCD) were infected with adeno-associated virus serotype 2 carrying DUSP26 short-hairpin RNA to examine the effects of DUSP26 silencing on aortic valve calcification. DUSP26 silencing ameliorated aortic valve calcification in HCD-treated ApoE$^{-/-}$ mice, as evidenced by reduced thickness and calcium deposition in the aortic valve leaflets, improved echocardiographic parameters (decreased peak transvalvular jet velocity and mean transvalvular pressure gradient, as well as increased aortic valve area), and decreased levels of osteogenic markers (Runx2, osterix, and osteocalcin) in the aortic valves. These results were confirmed in osteogenic medium-induced human valvular interstitial cells. Immunoprecipitation, liquid chromatography-tandem mass spectrometry, and functional assays revealed that dipeptidyl peptidase-4 (DPP4) interacted with DUSP26 to mediate the procalcific effects of DUSP26. High N^6-methyladenosine levels up-regulated DUSP26 in CAVD; in turn, DUSP26 activated DPP4 by antagonizing mouse double minute 2-mediated ubiquitination and degradation of DPP4, thereby promoting CAVD progression.

Conclusion DUSP26 promotes aortic valve calcification by inhibiting DPP4 degradation. Our findings identify a previously unrecognized mechanism of DPP4 up-regulation in CAVD, suggesting that DUSP26 silencing or inhibition is a viable therapeutic strategy to impede CAVD progression.

* Corresponding author. Email: dongnianguodoc@hotmail.com (N.D.); Email: wind8828@gmail.com (F.C.); Tel: +86 10 55499138, Email: jinxinunion@hust.edu.cn (X.J.)
† These authors contributed equally to this work and should be considered as co-first authors.

Graphical Abstract

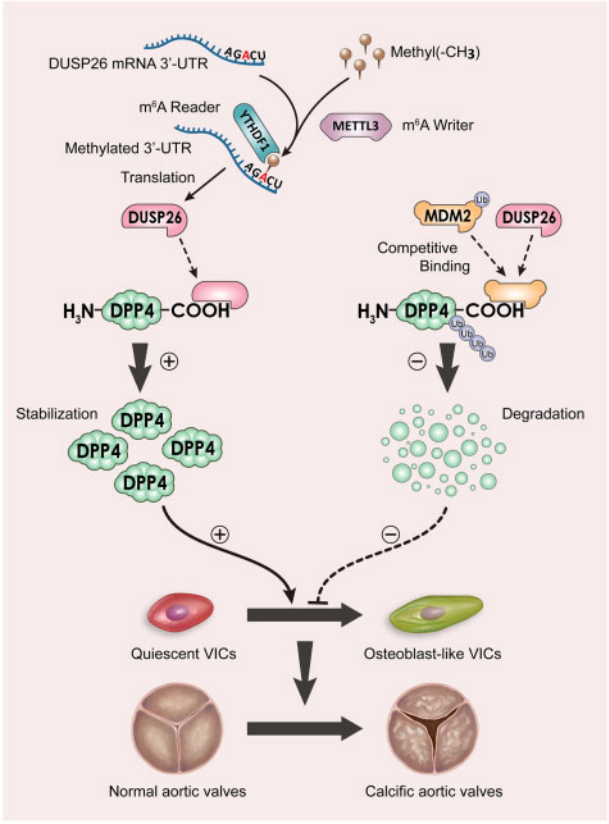

High m6A levels up-regulated DUSP26 in CAVD; in turn, DUSP26 enhanced DPP4 expression by antagonizing MDM2-mediated ubiquitination and degradation of DPP4, thereby promoting CAVD progression.

Keywords Dual-specificity phosphatase 26 • N^6-methyladenosine • Dipeptidyl peptidase-4 • Calcific aortic valve disease

Translational Perspective

Calcific aortic valve disease (CAVD) is a prevalent disorder with high morbidity and mortality rates and limited treatment options. Thus, there is an unmet medical need to identify novel therapeutic targets for CAVD. Our findings reveal a novel role of dual-specificity phosphatase 26 (DUSP26) in CAVD, independent of its phosphatase function. DUSP26 up-regulation is mediated by N^6-methyladenosine modification and promotes aortic valve calcification *in vitro* and *in vivo*. DUSP26 increases dipeptidyl peptidase-4 (DPP4) protein stability by preventing mouse double minute 2-induced DPP4 ubiquitination and degradation. Hence, DUSP26 depletion may represent a novel therapeutic strategy for CAVD.

Introduction

Calcific aortic valve disease (CAVD) is burdened by high morbidity and mortality associated with aortic sclerosis and stenosis.[1] Currently, there is no pharmacological treatment for CAVD; interventions targeting CAVD risk factors, such as lipid-lowering therapy, fail to suppress CAVD progression.[2] Surgical and transcatheter aortic valve replacement remain the most effective treatment options; however, they often cause complications and provide poor long-term outcomes. Therefore, research for identifying more suitable therapeutic options is ongoing. The phenotypic switching of human aortic valve interstitial cells (hVICs) to an osteoblast-like phenotype is recognized as the fundamental hallmark of valvular calcification.[3] Thus, effective strategies to prevent the osteogenic differentiation of hVICs may provide novel therapeutic options for CAVD.

Dual-specificity protein phosphatases (DUSPs), also known as mitogen-activated protein kinase (MAPK) phosphatases, are protein

tyrosine phosphatases that dephosphorylate threonine and tyrosine residues.[4] DUSPs have been implicated in atherosclerosis,[5,6] which has a similar aetiology to that of CAVD. Dual-specificity phosphatase 26 (DUSP26), a DUSP family member, regulates cell proliferation by dephosphorylating fas-associated protein with death domain[7] and has been proposed as a transforming growth factor beta-activated kinase 1 (TAK1)-targeted therapeutic option for nonalcoholic fatty liver disease.[8] Gómez-Banoy *et al.*[9] reported that DUSP26 inhibition alleviated type 2 diabetes. Furthermore, DUSP26 has been implicated in p38 MAPK-dependent regulation of neonatal cardiomyocyte proliferation in the mouse heart.[10] Nonetheless, the role of DUSP26 in CAVD remains unknown.

Dipeptidyl peptidase-4 (DPP4; also known as CD26) is a membrane-bound enzyme widely expressed in different organs.[11] DPP4 has been proposed as a therapeutic target for cardiometabolic diseases, such as atherosclerosis,[12] type 2 diabetes,[13] and CAVD.[14] We have recently shown that DPP4 regulates osteogenic differentiation in hVICs.[15] Nevertheless, DPP4 has various biological functions, and DPP4 inhibition may increase the risk of heart failure,[16] bullous pemphigoid,[17] and arthralgia.[18] Therefore, a better understanding of the role of DPP4 may lead to the development of effective therapies for CAVD.

In this study, we conducted tissue microarrays and found that DUSP26 was highly expressed in human calcific aortic valves (CAVs). DUSP26 up-regulation was mediated by N^6-methyladenosine (m^6A) modification in hVICs and was associated with CAVD progression *in vitro* and *in vivo*. By binding to its C-terminal domain, DUSP26 inhibited mouse double minute 2 (MDM2)-induced DPP4 ubiquitination and degradation in hVICs. Hence, DUSP26 depletion may represent a novel therapeutic strategy for CAVD.

Methods

Detailed methods are described in the Supplementary material online.

Human studies and ethics

Human-calcified aortic valve leaflets were obtained from patients with CAVD during aortic valve replacement. Control noncalcified aortic valves were collected from the explanted hearts of patients who underwent heart transplantation for dilated cardiomyopathy. Exclusion criteria included bicuspid aortic valves (BAVs), valves with moderate-to-severe aortic valve regurgitation, infective endocarditis, congenital valve disease, and rheumatic aortic valvulopathy. The protocol for this study complied with the Declaration of Helsinki and was approved by the Tongji Medical College Institutional Review Board, Huazhong University of Science and Technology. Written informed consent was obtained from all patients.

Animal studies and ethics

All animal experiments were approved by the Animal Care and Use Committee of Tongji Medical College and complied with the European Communities Council Directive 86/609/EEC and 2010/63/EU for the protection of animals used for experimental purposes. Male $ApoE^{-/-}$ C57BL/6 mice were used in this study as previously described.[15] Adeno-associated virus subtype 2 carrying short-hairpin RNA (shRNA) targeting DUSP26 (AAV2-sh-DUSP26) and AAV2-scramble (AAV2-scr) was delivered into 4-week-old $ApoE^{-/-}$ mice through the tail vein 4 weeks prior to diet treatment. $ApoE^{-/-}$ mice (8 weeks old) were randomly allocated into the following four groups and observed for 24 weeks: mice fed a normal diet (ND) and administered AAV2-sh-DUSP26 (n = 10); mice fed an ND and administered AAV2-scr ($n = 10$); mice fed a 0.25% high cholesterol diet (HCD; TD 88137, Harlan Teklad, Madison, WI, USA) and administered AAV2-sh-DUSP26 ($n = 10$); and mice fed an HCD and administered AAV2-scr ($n = 10$). HCD-fed animals were maintained on the diet for 24 weeks to induce aortic valve calcification.[15,19] Following final transthoracic echocardiography and haemodynamic assessment, mice were sacrificed, and aortic valves and blood were collected for histopathological examination.

Results

DUSP26 is up-regulated in human calcific aortic valves due to m^6A modification

To identify genes involved in CAVD, we analysed the gene expression profiles of three human CAVs and three normal aortic valves (see Supplementary material online, *Table S1* for the baseline characteristics of patients). We identified 401 differentially expressed genes in CAVs, with 215 up-regulated and 186 down-regulated genes (dataset 1) (filtered by |fold change (FC)| ≥ 2 and $P < 0.05$). The top 10 differentially expressed genes were evaluated by hierarchical clustering (*Figure 1A* and Supplementary material online, *Table S2*). To identify genes with functional significance from the top 10 up-regulated genes, we first verified their gene expression levels in 100 human aortic valves (50 CAVs and 50 normal controls; see Supplementary material online, *Table S3* for patient characteristics and Supplementary material online, *Figure S1* for calcification staining). Eight out of 10 of these genes were up-regulated in CAVs (Supplementary material online, *Figure S2A–J*). Functional shRNA screening to identify calcification-associated genes revealed that silencing of CBLN1, DUSP26, and LRRTM1 down-regulated three osteogenic markers (Runx2, osterix, and osteocalcin) in osteogenic medium-induced hVICs; DUSP26 silencing was the most prominent (Supplementary material online, *Figure S2K–M*). Hence, we focused on DUSP26 in our subsequent experiments. DUSP26 up-regulation in CAVs (*Figure 1B*) was confirmed by immunofluorescence staining (*Figure 1C*) and immunoblotting (*Figure 1D*). Interestingly, the DUSP26 protein preferentially accumulated on the aortic surface and not the ventricular surface of the leaflets. This localization indicates a potential role for DUSP26 in valvular calcification as calcification usually arises from the aortic side of the valve leaflets.[1]

We have previously shown that methyltransferase-like 3 (METTL3)-mediated m^6A modification accounts for the elevated expression of twist-related protein 1 (TWIST1) in CAVD.[20] To assess the relevance of m^6A in DUSP26 up-regulation, we analysed DUSP26 sequence and identified a consensus METTL3 motif (AGACU) in the 3′-untranslated region (3′-UTR) of DUSP26 mRNA adjacent to the stop codon (*Figure 1E and F* and Supplementary material online, *Figure S3*). m^6A dot blot analysis showed that the global m^6A level was increased in human CAVs (Supplementary material online, *Figure S4A*). In addition, osteogenic stimulation increased the global m^6A level in primary hVICs, which was attenuated and aggravated by METTL3 silencing and overexpression, respectively (*Figure 1G*). Importantly, RNA immunoprecipitation following quantitative real-time polymerase chain reaction (RIP-qRT-PCR) showed that METTL3 directly interacted with DUSP26 mRNA (*Figure 1H*)

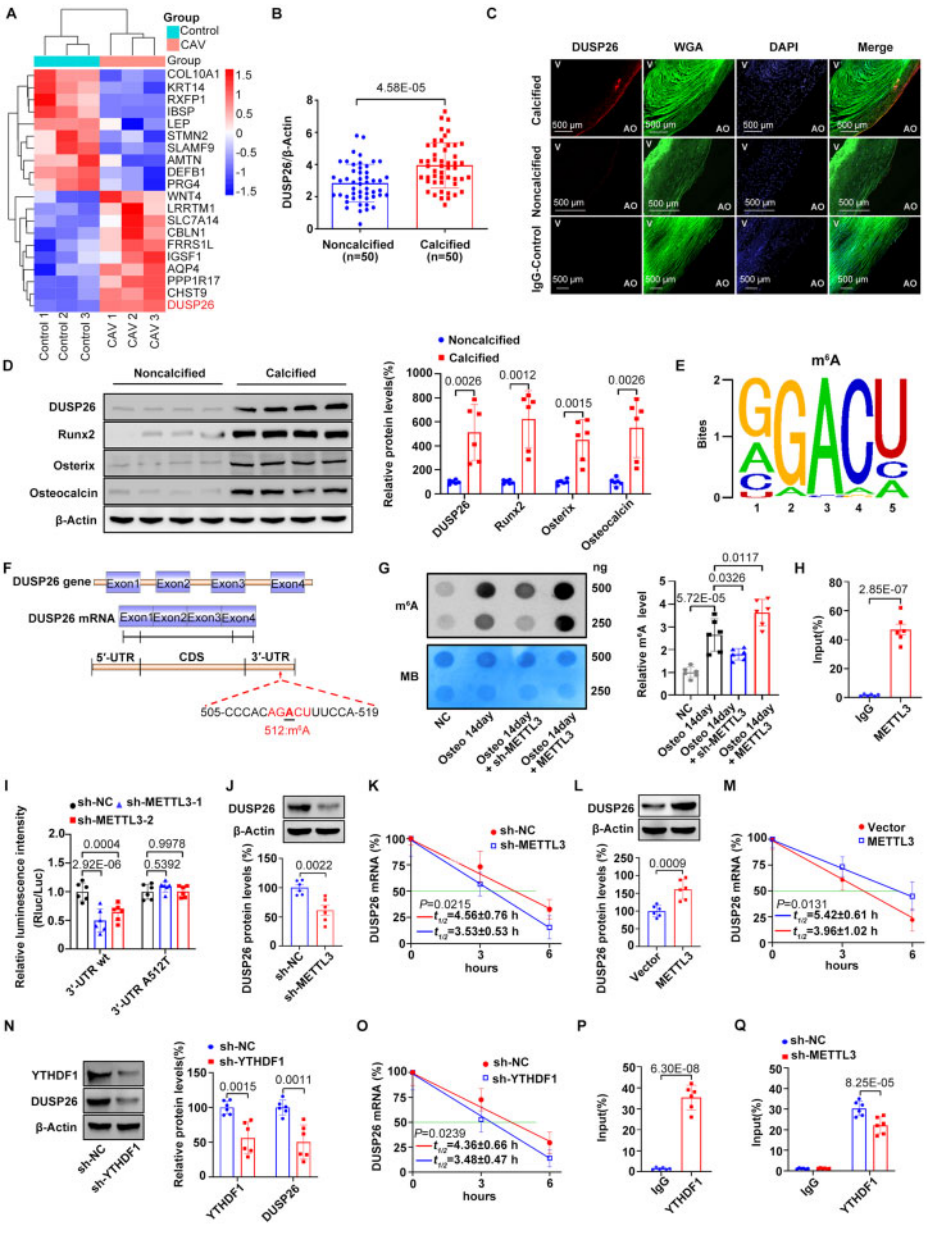

Figure 1 DUSP26 is up-regulated in human calcific aortic valves and undergoes METTL3-mediated m^{6}A modification. (*A*) Heatmap showing the top 10 differentially expressed genes in human aortic valve samples. (*B*) DUSP26 mRNA levels in aortic valves from patients with CAVD and normal controls. Unpaired two-tailed Student's *t*-test, $n = 50$ per group. DUSP26 protein levels in human aortic valves were determined by immunofluorescence (*C*) and Western blot (*D*). Unpaired two-tailed Student's *t*-test, $n = 6$ per group. Corrected for multiple comparisons using the Holm–Sidak method (four tests). (*E*) The consensus motif of METTL3 (AGACU) targeting the 3′-UTR of DUSP26 mRNA for m^{6}A modification. (*F*) The location of the m^{6}A site in the DUSP26 mRNA. (*G*) The m^{6}A level of poly(A) + RNAs isolated from total RNA of hVICs. Methylene blue staining served as a loading control. One-way ANOVA followed by Bonferroni *post hoc* test. (*H*) The interaction between the METTL3 protein and DUSP26 mRNA in hVICs was measured by RNA immunoprecipitation followed by qRT-PCR analysis. Unpaired two-tailed Student's *t*-test, $n = 6$ per group. (*I*) Luciferase activities of the wild-type (wt) and mutated DUSP26 3′-UTR reporters in hVICs that were transfected with wt or mutated pmiR-RB-Report-DUSP26-3′UTR plasmids. Two-way ANOVA followed by Bonferroni *post hoc* test. (*J*) DUSP26 protein levels in hVICs transfected with shRNA targeting METTL3. Unpaired two-tailed Student's *t*-test, $n = 6$ per group. (*K*) DUSP26 RNA stability in METTL3-knockdown hVICs was measured by one-phase decay analysis. (*L*) DUSP26 protein levels in hVICs overexpressing METTL3. Unpaired two-tailed Student's *t*-test, $n = 6$ per group. (*M*) DUSP26 RNA stability in METTL3 overexpressing hVICs was measured by one-phase decay analysis. (*N*) The protein levels of DUSP26 and YTHDF1 in YTHDF1-knockdown hVICs. Unpaired two-tailed Student's *t*-test, $n = 6$ per group. Corrected for multiple comparisons using the Holm-Sidak method (2 tests). (*O*) DUSP26 RNA stability in YTHDF1-knockdown hVICs was measured by one-phase decay analysis. (*P*) The interaction between the YTHDF1 protein and DUSP26 mRNA in hVICs was measured by RIP followed by qRT-PCR analysis. Unpaired two-tailed Student's *t*-test, $n = 6$ per group. (*Q*) The interaction between the YTHDF1 protein and DUSP26 mRNA in METTL3-knockdown hVICs was measured by RIP followed by qRT-PCR analysis. Two-way ANOVA followed by Bonferroni *post hoc* test. Scale bar: 500 μm. Values are mean ± SD.

and that METTL3 silencing significantly decreased m^{6}A levels of DUSP26 mRNA in hVICs (Supplementary material online, *Figure S4B*). METTL3 silencing decreased while METTL3 overexpression increased the luciferase activity of the wild-type DUSP26 3′-UTR reporter (*Figure 1I* and Supplementary material online, *Figure S4C*). However, neither knockdown nor overexpression of METTL3 altered the luciferase activity of the mutated DUSP26 3′-UTR reporter (*Figure 1I* and Supplementary material online, *Figure S4C*). METTL3 depletion significantly reduced DUSP26 protein levels and its mRNA half-life (*Figure 1J and K*). Conversely, METTL3 overexpression increased DUSP26 protein levels and DUSP26 mRNA half-life (*Figure 1L and M*). These findings suggest that METTL3-mediated m^{6}A modification accounts for the increased expression of DUSP26 in CAVD by enhancing its mRNA stability.

METTL3 has been shown to promote the translation of its targets in a YTH domain family 1 (YTHDF1)-mediated m^{6}A-dependent manner.[21,22] Therefore, we further explored the role of YTHDF1 in the translation of m^{6}A-methylated DUSP26 in hVICs. YTHDF1 depletion reduced DUSP26 protein levels and DUSP26 mRNA half-life (*Figure 1N and O*), while YTHDF1 overexpression had the opposite effects (Supplementary material online, *Figure S4D* and *E*). YTHDF1 directly interacted with DUSP26 mRNA (*Figure 1P*); this interaction was inhibited or strengthened by METTL3 silencing (*Figure 1Q*) or overexpression (Supplementary material online, *Figure S4F*), respectively. Taken together, these data suggested that METTL3 facilitates the translation of m^{6}A-methylated DUSP26 mRNA in a YTHDF1-dependent manner.

DUSP26 ablation ameliorates aortic valve calcification *in vivo*

To investigate the role of DUSP26 in aortic valve calcification *in vivo*, we silenced DUSP26 expression in ApoE$^{-/-}$ mice using AAV2-sh-DUSP26 (or AAV2-scr control) delivered via tail vein injection.[23] The efficiency of DUSP26 silencing in the aortic valves was validated (Supplementary material online, *Figure S5*). After 24 weeks, the mice in the HCD + AAV2-scr group showed significant increases in peak transvalvular jet velocity (*Figure 2A*) and mean transvalvular pressure gradient (*Figure 2B*) and a significant decrease in aortic valve area (AVA; *Figure 2C*); DUSP26 knockdown partly restored these changes (*Figure 2A–C*). However, there were no significant differences in left ventricular/right ventricular diameters, left ventricular systolic/diastolic function, haemodynamic parameters, or arterial blood pressure between the HCD groups (Supplementary *Table 4*). Left ventricular global longitudinal strain (GLS) analysis showed that HCD slightly decreased GLS; however, this change was not significant (Supplementary *Table 4*). Insignificant trends towards higher GLS were also observed in the HCD+AAV2-sh-DUSP26 group in comparison to the HCD+AAV2-scr group (Supplementary *Table 4*). We also found no significant changes in mean pulmonary arterial pressure, right ventricle/(left ventricle + interventricular septum), cross-sectional area of the right ventricle (Supplementary material online, *Figure S6A–C*) and haemodynamic parameters (Supplementary *Table 5*) between the four groups. These data suggest an insignificant role for DUSP26 in pulmonary hypertension and right ventricular morphology and function.

We then examined valve leaflet morphology, fibrosis, and calcification in ApoE$^{-/-}$ mice. HCD promoted aortic valve calcification in ApoE$^{-/-}$ mice as evidenced by increased aortic valve leaflet thickness (*Figure 2D*) and collagen (*Figure 2E*) and calcium deposition (*Figure 2F and G*). Strikingly, DUSP26 silencing partially normalized these changes (*Figure 2D–G*) and reduced the levels of osteogenic markers (*Figure 2H*). However, DUSP26 silencing failed to significantly modulate the levels of glucose, total cholesterol, low-density lipoprotein, and triglycerides (Supplementary material online, *Table 6*). These results suggest that DUSP26 silencing ameliorates aortic valve calcification in ApoE$^{-/-}$ mice independently of metabolic regulation. Osteoprogenitor cells (OPCs) have been shown to promote ectopic calcification, including aortic valve calcification.[24,25] DUSP26 silencing failed to alter the proportion of circulating OPCs (Supplementary material online, *Figure S7*), suggesting that OPCs may not contribute to DUSP26-mediated aortic valve calcification in ApoE$^{-/-}$ mice.

DUSP26 silencing ameliorates aortic valve calcification *in vitro*

As the phenotypic transformation of hVICs into osteoblast-like cells is a critical step in CAVD pathogenesis,[15,19] we investigated whether DUSP26 orchestrated hVIC osteogenic differentiation. We isolated hVICs from human aortic valves from non-CAVD controls (see Supplementary *Table 7* for patient characteristics and Supplementary material online, *Figure S8* for the identification of primary hVICs). Before osteogenic induction, the protein levels of osteogenic markers and calcium deposition were undetectable in hVICs (Supplementary material online, *Figure S9*). Thus, hVICs were maintained in a quiescent state before commencing the experiments, as previously described.[26] We exposed hVICs to osteogenic medium to stimulate osteogenic differentiation;[19] osteogenic induction was accompanied by time-dependent increases in DUSP26 mRNA and protein levels (*Figure 3A and B*), along with Runx2 up-regulation (*Figure 3B*). Positive correlations between the mRNA levels of DUSP26 and osteogenic markers were revealed (Runx2, $r = 0.5236$, $P = 0.0003$; osterix, $r = 0.6605$, $P = 0.0001$; osteocalcin, $r = 0.5397$, $P = 0.0002$; Supplementary material online, *Figure S10*).

Next, we investigated whether DUSP26 could reprogram hVICs towards an osteogenic phenotype. DUSP26 silencing negated the osteogenic medium-induced increase in the levels of osteogenic markers (*Figure 3C*), calcified nodule formation, and calcium deposition (*Figure 3D* and Supplementary material online, *Figure S11*); DUSP26 overexpression had the opposite effects (*Figure 3E and F*). We also isolated hVICs from human aortic valve tissues from CAVD patients (see Supplementary *Table 7* for patient characteristics). We compared the phenotype of hVICs from CAVD patients and non-CAVD controls at baseline and found that only hVICs from CAVD patients exhibited calcium deposition and expression of osteogenic markers (Supplementary material online, *Figure S12*), indicating that osteogenic changes in hVICs are characteristic features of CAVD patients.[14,27] Furthermore, the effects of DUSP26 manipulation in hVICs from CAVD patients were similar to those in hVICs from non-CAVD controls (*Figure 3*).

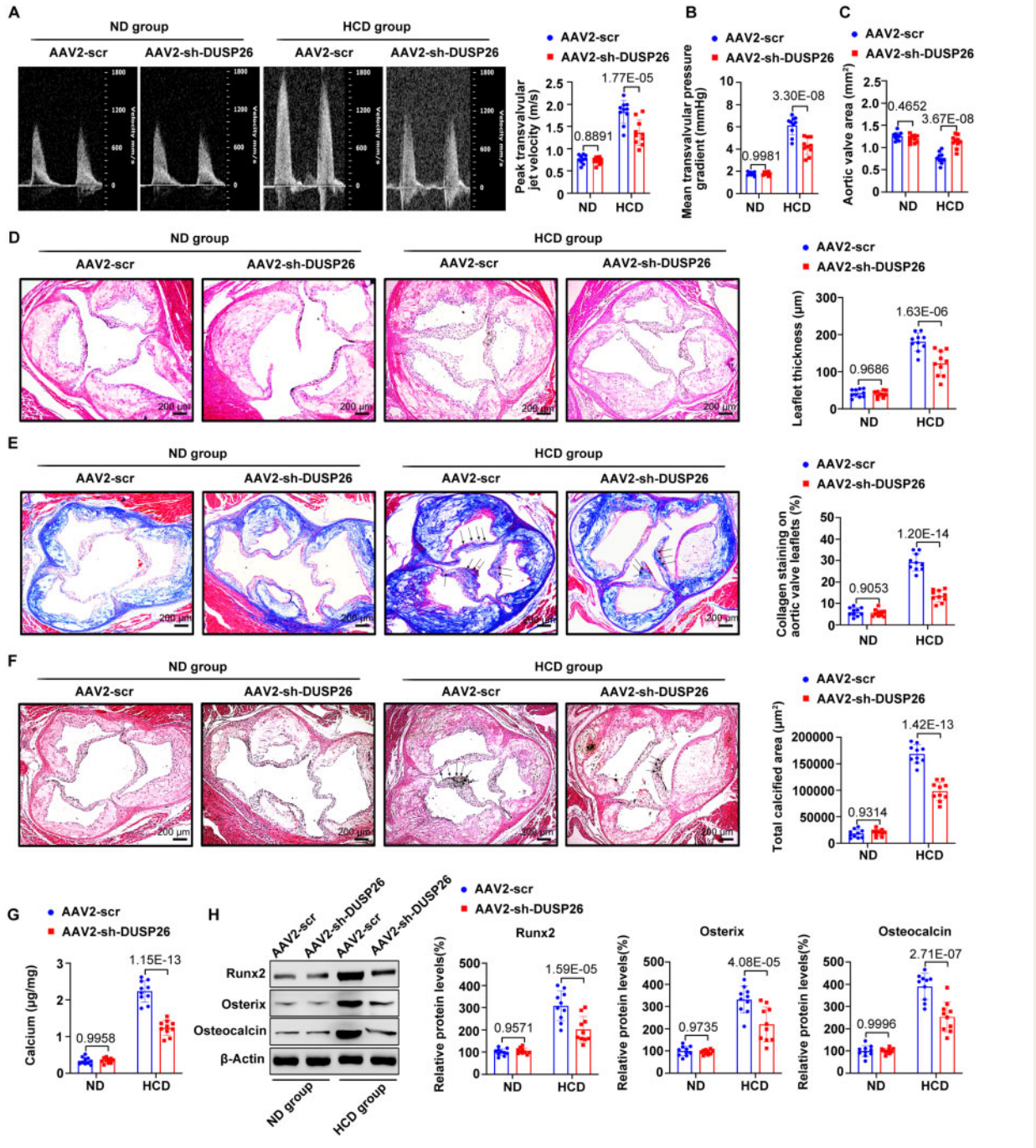

Figure 2 DUSP26 deletion alleviates aortic valve calcification *in vivo*. Echocardiographic data in ApoE$^{-/-}$ mice. (*A*) peak transvalvular jet velocity, (*B*) mean transvalvular pressure gradient, and (*C*) AVA. (*D*) Haematoxylin and eosin staining of aortic valve leaflets from ApoE$^{-/-}$ mice. (*E*) Masson's trichrome staining of aortic valve leaflets from ApoE$^{-/-}$ mice. (*F*) Von Kossa staining of aortic valve leaflets from ApoE$^{-/-}$ mice. (*G*) The calcium content of aortic valve leaflets from ApoE$^{-/-}$ mice. (*H*) The protein levels of three osteogenic markers (Runx2, osterix, and osteocalcin) in aortic valve leaflets from ApoE$^{-/-}$ mice. Two-way ANOVA followed by Bonferroni *post hoc* test. $n = 10$ per group. Scale bar: 200 μm. Values are the mean ± SD.

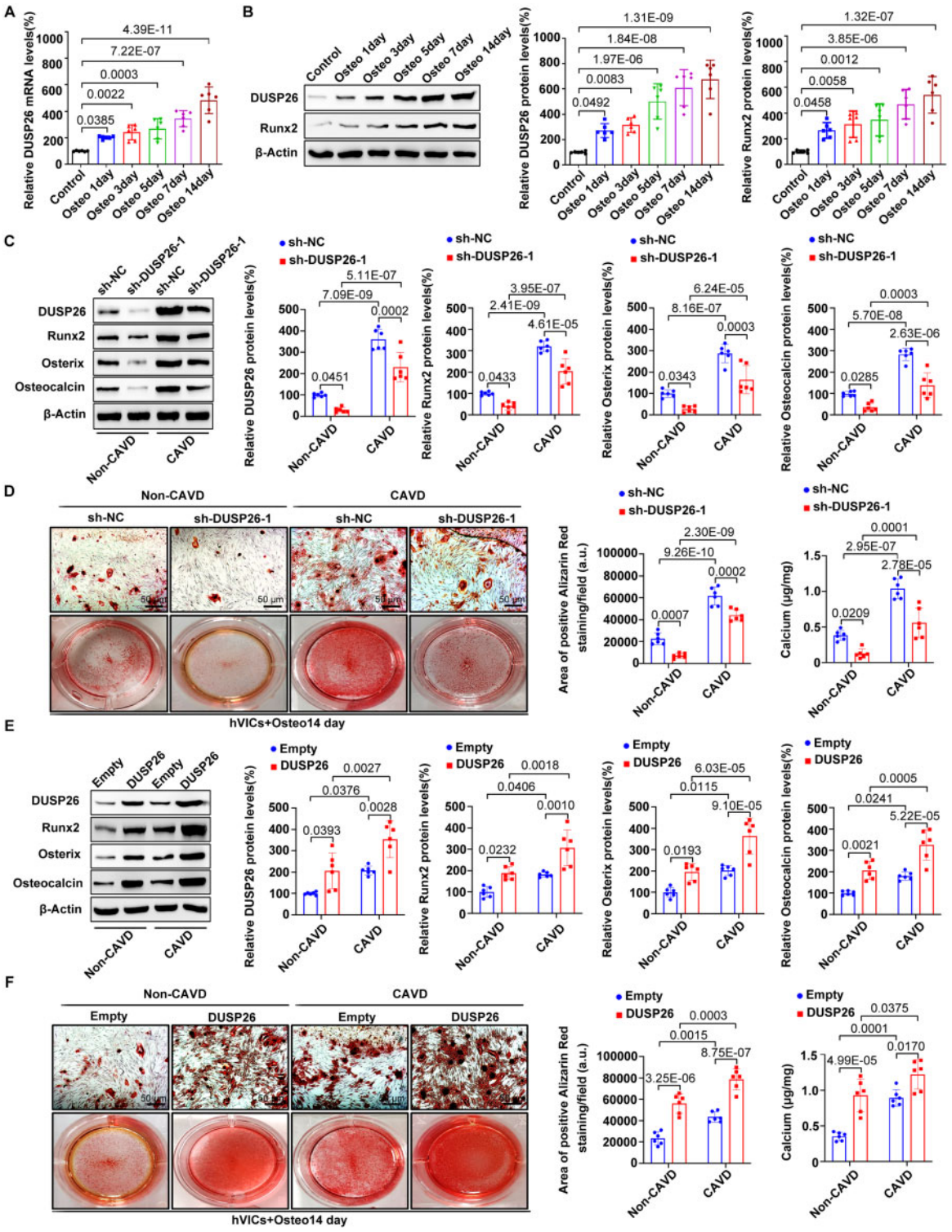

Figure 3 DUSP26 promotes osteogenic differentiation in hVICs. DUSP26 mRNA (*A*) and protein (*B*) levels in hVICs harvested at different time points (days 0, 1, 3, 5, 7, and 14). One-way ANOVA followed by Bonferroni *post hoc* test. (*C*) HVICs isolated from human-calcified and noncalcified aortic valves were transfected with shRNA targeting DUSP26. Protein levels of DUSP26 and three osteogenic markers (Runx2, osterix, and osteocalcin) in calcified and noncalcified hVICs. Two-way ANOVA followed by Bonferroni *post hoc* test. (*D*) Alizarin red staining of mineralization nodules in calcified and noncalcified hVICs following DUSP26 silencing. Two-way ANOVA followed by Bonferroni *post hoc* test. (*E*) Protein levels of DUSP26 and three osteogenic markers and (*F*) Alizarin red staining of mineralization nodules in calcified and noncalcified hVICs overexpressing DUSP26. Two-way ANOVA followed by Bonferroni *post hoc* test. $n = 6$ per group. Scale bar: 50 μm. Values are mean ± SD.

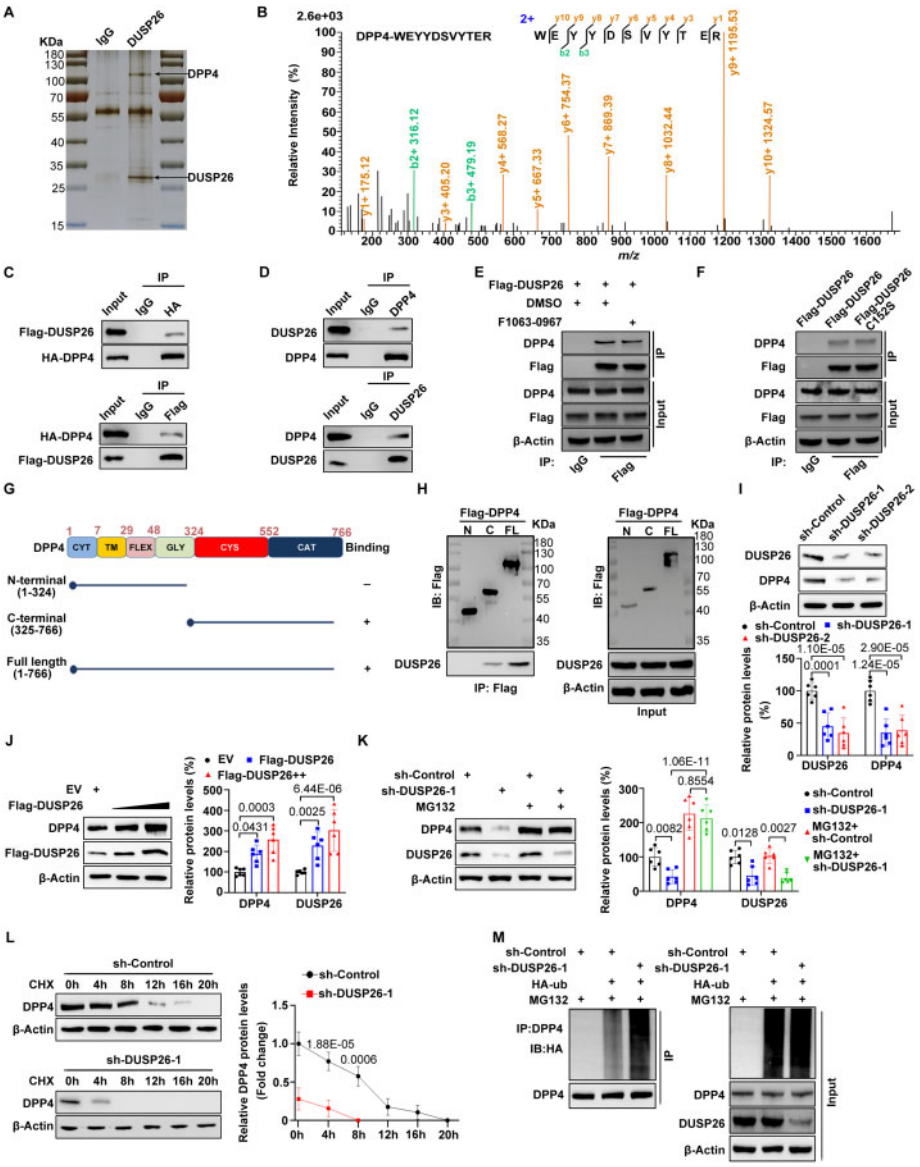

Figure 4 DUSP26 interacts with DPP4 and protects it from ubiquitin-mediated degradation in hVICs. (*A*) Silver-stained gel of total protein from hVICs after immunoprecipitation with IgG or anti-DUSP26 antibody. (*B*) DPP4 peptides derived from the mass spectrometric analysis of DUSP26. (*C*) Co-immunoprecipitation (co-IP) to detect the interaction between HA-tagged DPP4 (HA-DPP4) and Flag-tagged DUSP26 (Flag-DUSP26). The protein lysates isolated from hVICs co-transfected with HA-DPP4 and Flag-DUSP26 were immunoprecipitated with anti-HA antibody and were immunoblotted with anti-Flag antibody (upper panel), or immunoprecipitated with anti-Flag antibody and immunoblotted with anti-HA antibody (lower panel). (*D*) Co-IP to detect the interaction between endogenous DPP4 and DUSP26. Protein lysates from hVICs were immunoprecipitated with anti-DPP4 antibody and immunoblotted with anti-DUSP26 antibody (upper panel), or immunoprecipitated with anti-DUSP26 antibody and immunoblotted with anti-DPP4 antibody (lower panel). (*E*) Co-IP to detect the interaction between DPP4 and Flag-DUSP26. HVICs were transfected with Flag-DUSP26 and treated with or without 20 μmol/L F1063-0967. The protein lysates of hVICs were immunoprecipitated with anti-Flag antibody and immunoblotted with the indicated antibodies. (*F*) Co-IP to detect the interaction between DPP4 and Flag-DUSP26. The protein lysates isolated from the hVICs transfected with Flag-DUSP26 wild-type or its phosphatase-dead mutant (Flag-DUSP26 C152S) were immunoprecipitated with anti-Flag antibody and immunoblotted with the indicated antibodies. (*G*) Schematic representation of the DPP4 domain. (*H*) Co-IP to detect the interaction between DUSP26 and Flag-DPP4. hVICs were transfected with Flag-tagged wild-type full-length DPP4 (Flag-DPP4 FL), truncation of DPP4 C-terminal 325–766 aa (Flag-DPP4 N), or 1–324 aa (Flag-DPP4 C) for 24 h. Protein lysates were immunoprecipitated with anti-Flag antibody and immunoblotted with the indicated antibodies. (*I–J*) Western blot analysis of hVICs transfected with Flag-DUSP26 or empty vector (EV). One-way ANOVA followed by Bonferroni *post hoc* test. (*K*) HVICs were infected with sh-DUSP26-1 or sh-Control for 48 h. Before immunoblotting, cells were treated with the 26S proteasome inhibitor MG132 for 8 h. One-way ANOVA followed by Bonferroni *post hoc* test. (*L*) Western blot analysis of DPP4 and β-Actin in hVICs transfected with sh-DUSP26-1 or sh-Control for 48 h, then treated with cycloheximide (CHX) for 0, 4, 8, 12, 16, and 20 h. Two-way ANOVA followed by Bonferroni *post hoc* test. (*M*) Co-IP to detect DPP4 ubiquitination. HVICs were transfected with the indicated shRNAs for 48 h and treated with MG132 for 8 h. The protein lysates were immunoprecipitated with an anti-DPP4 antibody and immunoblotted with the indicated antibodies. Values are mean ± SD.

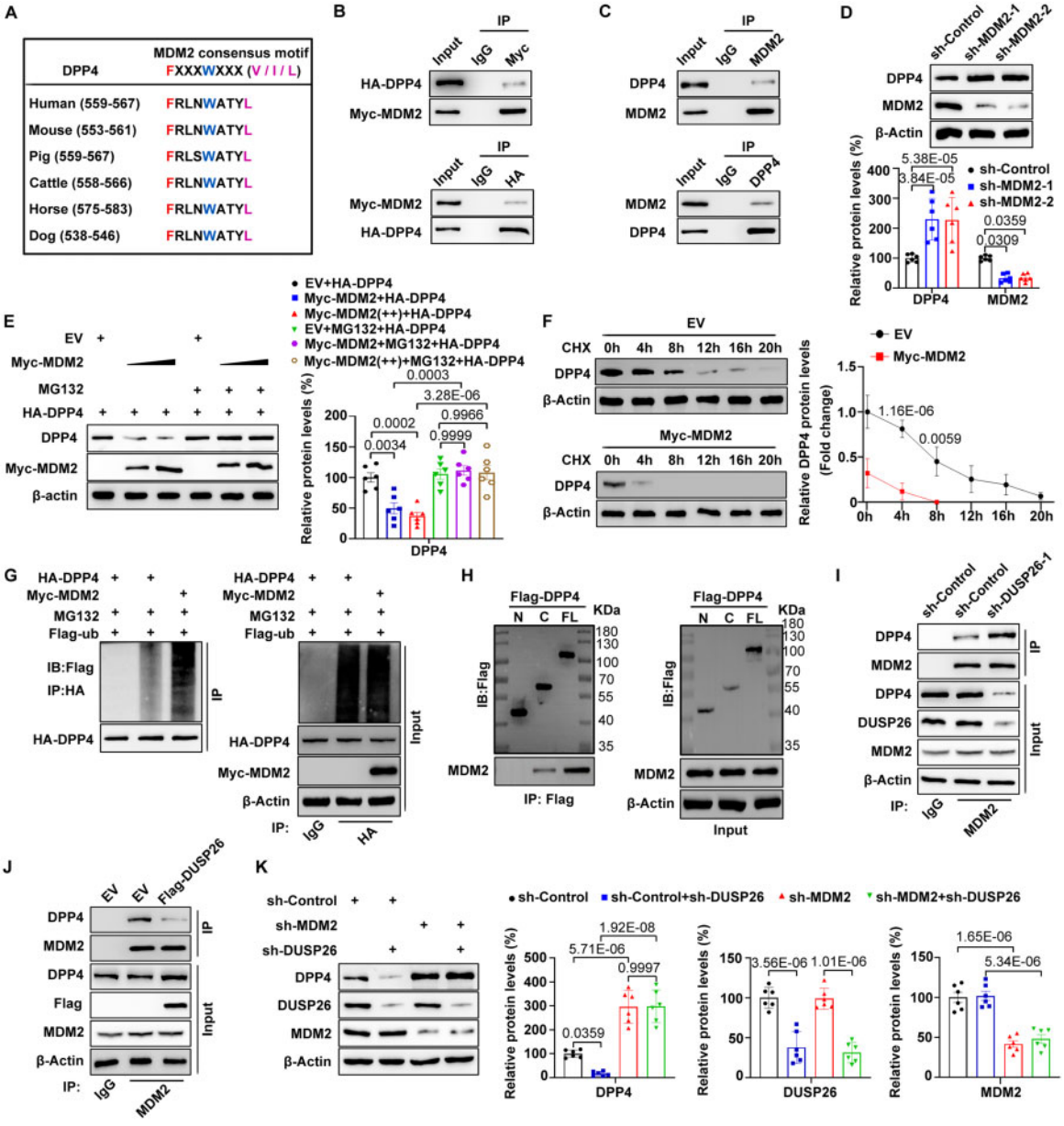

Figure 5 DUSP26 stabilizes DPP4 by competing with MDM2-mediated ubiquitination in hVICs. (*A*) Schematic diagram depicting the conserved MDM2-binding motif in the DPP4 protein. (*B*) Co-immunoprecipitation (co-IP) to detect the interaction between HA-tagged DPP4 (HA-DPP4) and Myc-tagged MDM2 (Myc-MDM2). The protein lysates from hVICs co-transfected with HA-DPP4 and Myc-MDM2 were immunoprecipitated with anti-Myc antibody and immunoblotted with anti-HA antibody (upper panel), or they were immunoprecipitated with anti-HA antibody and immunoblotted with anti-Myc antibody (lower panel). (*C*) Co-IP to detect the interaction between endogenous DPP4 and MDM2. The protein lysates isolated from hVICs were immunoprecipitated with anti-MDM2 antibody and immunoblotted with anti-DPP4 antibody (upper panel), or immunoprecipitated with anti-DPP4 antibody and immunoblotted with anti-MDM2 antibody (lower panel). (*D* and *E*) Western blot analysis of hVICs after transfection with the indicated plasmids. One-way ANOVA followed by Bonferroni *post hoc* test. (*F*) Western blot analysis of DPP4 and β-Actin in hVICs transfected with Myc-MDM2 or empty vector (EV) for 48 h and treated with cycloheximide (CHX) for 0, 4, 8, 12, 16, and 20 h. Two-way ANOVA followed by Bonferroni *post hoc* test. (*G*) Co-IP to detect ubiquitination of HA-DPP4. HVICs were co-transfected with HA-DPP4 or Myc-MDM2 for 24 h and treated with MG132 for 8 h. Protein lysates were immunoprecipitated with anti-HA antibody and immunoblotted with the indicated antibodies. (*H*) Co-IP to detect the interaction between MDM2 and Flag-DPP4. HVICs were transfected with Flag-tagged wild-type full-length DPP4 (Flag-DPP4 FL) or its truncated mutations 325–766 aa (Flag-DPP4 N) and 1–324 aa (Flag-DPP4 C) for 24 h. Protein lysates were immunoprecipitated with anti-Flag antibody and immunoblotted with the indicated antibodies. (*I* and *J*) Co-IP to detect the interaction between DPP4 and MDM2. The protein lysates isolated from hVICs transfected with the indicated shRNAs (*I*) or the indicated plasmids (*J*) were immunoprecipitated with anti-MDM2 and immunoblotted with the indicated antibodies. (*K*) Western blot analysis of hVICs transfected with the indicated shRNAs and plasmids. One-way ANOVA followed by Bonferroni *post hoc* test. Values are mean ± SD.

DUSP26 interacts with DPP4 and prevents its degradation in hVICs

HVIC extracts were immunoprecipitated with immunoglobulin G (IgG) or anti-DUSP26 antibody (*Figure 4A*) for mass spectrometry analysis. We identified DPP4 as a potential binding partner of DUSP26 in hVICs (*Figure 4B*). To verify this interaction, we co-transfected hVICs with HA-tagged DPP4 and Flag-tagged DUSP26 (*Figure 4C*). Coimmunoprecipitation (co-IP) analysis showed that exogenously overexpressed Flag-DUSP26 could bind HA-DPP4 in hVICs (*Figure 4C*). The interaction between endogenous DUSP26 and DPP4 was also verified in hVICs (*Figure 4D*). As DUSP26 acts as a protein phosphatase,[28] we explored whether its enzymatic activity was required for its interaction with DPP4. Treatment with the DUSP26 inhibitor F1063-0967[29] did not affect the interaction between DUSP26 and DPP4 in hVICs (*Figure 4E*). Similarly, the DUSP26 phosphatase-dead mutant (C152S) preserved its ability to bind DPP4 (*Figure 4F*). Thus, DUSP26 interacts with DPP4 independently of its phosphatase activity. Furthermore, we constructed DPP4-N-terminal (amino acids 1–324) and DPP4-C-terminal (amino acids 325–766) plasmids to determine which region of DPP4 interacted with DUSP26 (*Figure 4G*). DUSP26, full-length Flag-DPP4, N-terminal Flag-DPP4, and C-terminal Flag-DPP4 were translated *in vitro* as previously reported.[30] IP analyses revealed that the C-terminus of DPP4 interacted with DUSP26 (*Figure 4H*), suggesting that DUSP26 interacts with DPP4 by binding to the C-terminus of DPP4.

We also investigated the role of DUSP26 in DPP4 expression in hVICs. Intriguingly, DUSP26 knockdown decreased the protein level but not the mRNA level of DPP4 in hVICs (*Figure 4I* and Supplementary material online, *Figure S13A*). Conversely, DUSP26 overexpression increased the DPP4 protein level but not the mRNA level (*Figure 4J* and Supplementary material online, *Figure S13B*). Overexpression of phosphatase-dead mutant (C152S) DUSP26 also increased the protein level of DPP4 in hVICs (Supplementary material online, *Figure S13C*), suggesting that DUSP26 regulates DPP4 expression at the posttranslational level independent of its phosphatase activity. Poly-ubiquitination is a posttranscriptional modification promoting protein degradation *via* the 26S proteasome.[31] DUSP26 silencing-induced DPP4 down-regulation was attenuated by the 26S proteasome inhibitor MG132 (*Figure 4K*). Moreover, DUSP26 knockdown shortened the half-life of DPP4 and increased the polyubiquitination of DPP4 in hVICs (*Figure 4L and M*). Likewise, DUSP26 overexpression failed to further increase DPP4 levels upon MG132 treatment (Supplementary material online, *Figure S13D*). Further more, DUSP26 overexpression prolonged the half-life of DPP4 and reduced the polyubiquitination of DPP4 in hVICs (Supplementary material online, *Figure S13E* and *F*). DUSP26 levels were correlated with DPP4 levels in human CAVD samples ($r = 0.5096$, $P = 0.0217$; Supplementary material online, *Figure S14A*).

DUSP26 inhibits MDM2-mediated DPP4 ubiquitination in hVICs

We identified a conserved MDM2-binding motif in DPP4 protein (*Figure 5A*). To explore whether MDM2 functions as a novel E3 ligase of DPP4, we conducted co-IP to assess the interaction between DPP4 and MDM2. Ectopically expressed HA-DPP4 was coimmunoprecipitated by Myc-tagged MDM2 in hVICs (*Figure 5B*). The interaction between endogenous DPP4 and MDM2 was confirmed (*Figure 5C*). In addition, MDM2 silencing by two different shRNAs increased the protein level but not the mRNA level of DPP4 in hVICs (*Figure 5D* and Supplementary material online, *Figure S15*). Conversely, MDM2 overexpression decreased the protein level of DPP4 in hVICs, and this effect was inhibited by MG132 (*Figure 5E*). Furthermore, MDM2 overexpression reduced the half-life of DPP4 (*Figure 5F*) and increased DPP4 polyubiquitination in hVICs (*Figure 5G*). These data suggest DPP4 as a *bona fide* substrate of MDM2.

To identify the region of DPP4 responsible for MDM2 binding, we performed *in vitro* co-IP and found that the C-terminus of DPP4 interacted with MDM2 (*Figure 5H*). As the C-terminus of DPP4 interacted also with DUSP26 (*Figure 4H*), we explored the ability of DUSP26 to compete with MDM2 binding to DPP4 in hVICs. DUSP26 silencing in hVICs augmented the interaction between MDM2 and DPP4 (*Figure 5I*). In contrast, DUSP26 overexpression blocked the binding between MDM2 and DPP4 (*Figure 5J*). Moreover, DUSP26 knockdown decreased DPP4 protein levels; this effect was diminished upon co-knockdown of DUSP26 and MDM2 in hVICs (*Figure 5K*). We also found an inverse correlation between MDM2 and DUSP26 protein levels ($r = -0.5638$, $P = 0.0096$; Supplementary material online, *Figure S14B*). Likewise, a negative correlation was seen between MDM2 and DPP4 protein levels in 20 human CAVs ($r = -0.6569$, $P = 0.0017$; Supplementary material online, *Figure S14C*). These results suggest that MDM2 functions as a novel E3 ligase of DPP4, and DUSP26 competes with MDM2 binding to the C-terminus of DPP4, increasing DPP4 protein stability in hVICs.

DUSP26 exerts procalcific effects through DPP4 up-regulation

Next, we performed a rescue experiment to confirm whether DUSP26 functions through DPP4 up-regulation. The calcification alleviation effects of DUSP26 knockdown were reversed by DPP4 overexpression (*Figure 6A and B*). In contrast, the procalcific effects of DUSP26 overexpression were prevented by DPP4 depletion (*Figure 6C and D*), indicating that DUSP26 promotes osteogenic differentiation by up-regulating DPP4 in hVICs.

DPP4 inhibition alleviates aortic valve calcification *in vivo*

Sitagliptin, a selective DPP4 inhibitor, has been shown to reduce calcification in $eNOS^{-/-}$ mice.[14] Here, we orally administered HCD-fed $ApoE^{-/-}$ mice with vehicle or sitagliptin for 24 weeks. Sitagliptin ameliorated aortic valve calcification in HCD-fed $ApoE^{-/-}$ mice, as evidenced by improved echocardiographic parameters (decreased peak transvalvular jet velocity and mean transvalvular pressure gradient and increased AVA), reduced collagen and calcium deposition, and decreased levels of osteogenic markers in the aortic valve leaflets (Supplementary material online, *Figure S16*).

DUSP26 expression is associated with CAVD severity

To assess the clinical relevance of our findings, we analysed the correlation between DUSP26 levels and markers of subclinical atherosclerosis and CAVD severity in 50 human CAVs (validation cohort). The relationship between DUSP26 expression levels and CAVD

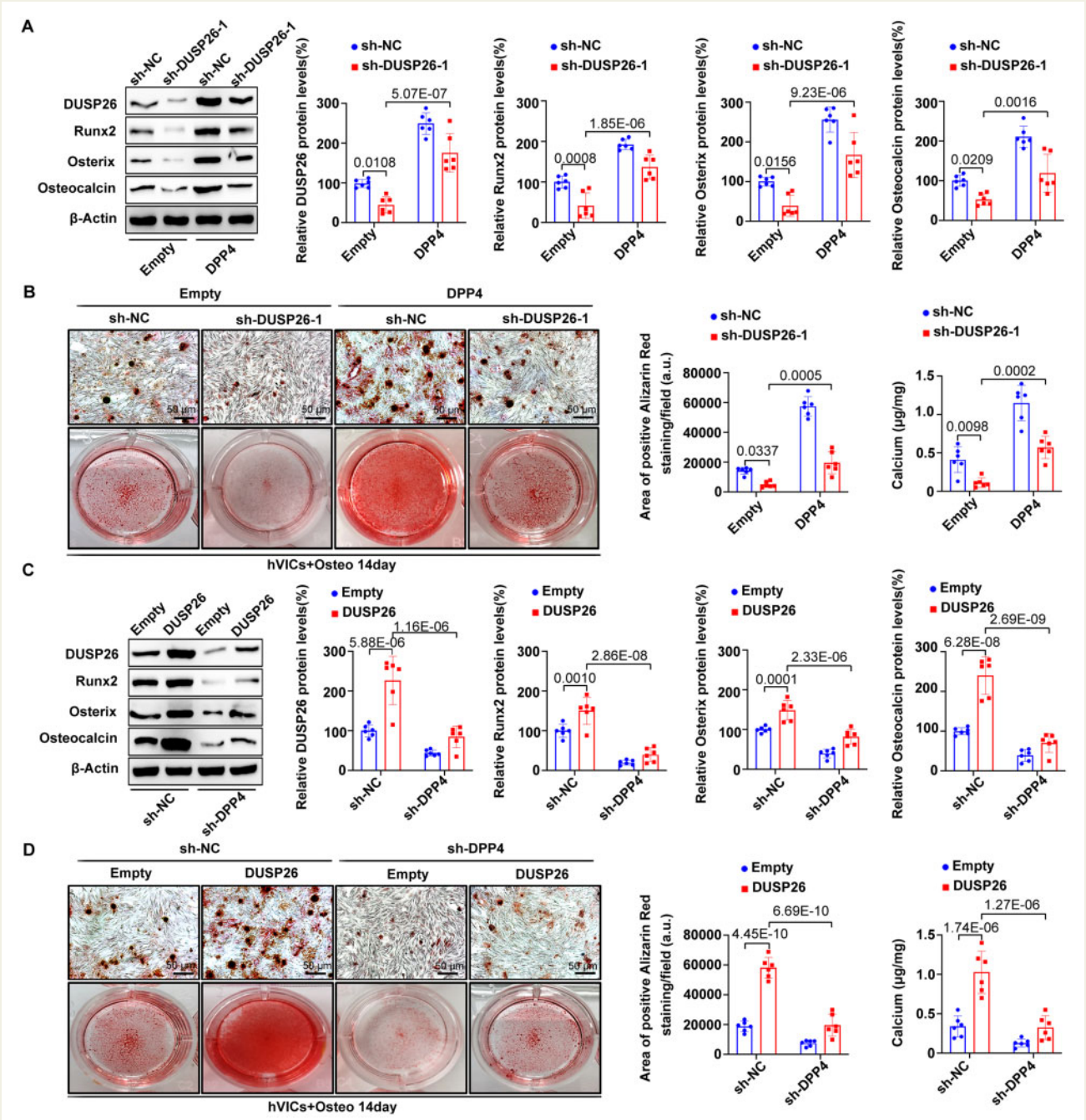

Figure 6 DPP4 overexpression rescues the osteogenic differentiation phenotypes induced by DUSP26 silencing in hVICs. (*A*) Western blot analysis of DUSP26 and three osteogenic markers (Runx2, osterix, and osteocalcin) in hVICs with DUSP26 silencing and DPP4 overexpression. Two-way ANOVA followed by Bonferroni *post hoc* test. (*B*) Alizarin red staining of mineralization nodules in hVICs with DUSP26 silencing and DPP4 overexpression. Two-way ANOVA followed by Bonferroni *post hoc* test. (*C*) The protein levels of DUSP26 and three osteogenic markers in hVICs with DUSP26 silencing and DPP4 overexpression. Two-way ANOVA followed by Bonferroni *post hoc* test. (*D*) Alizarin red staining of mineralization nodules in hVICs with DUSP26 silencing and DPP4 overexpression. Two-way ANOVA followed by Bonferroni *post hoc* test. $n = 6$ per group. Scale bar: 50 μm. Values are mean ± SD.

severity was consistent with the pro-calcification effect of DUSP26. Higher DUSP26 expression was associated with lower AVA, higher mean transvalvular pressure gradient, and higher peak transvalvular pressure gradient. However, DUSP26 levels were not significantly correlated with the carotid intima-media thickness and carotid plaque area (Supplementary material online, *Figure S17*).

Discussion

CAVD is a multifactorial disease with high spatiotemporal heterogeneity,[32] and its pathogenesis involves genetic factors, lipoprotein deposition, inflammation, and osteogenic transition of cardiac valve interstitial cells.[33] Although a few risk factors have been identified, the molecular mechanisms causing aortic valve calcification are poorly understood. Currently, there are no effective interventions that prevent CAVD progression.[34] This is the first study to show that DUSP26 promotes aortic valve calcification by up-regulating DPP4. Specifically, we found that increased DUSP26 levels in human aortic valves were associated with valve calcification. DUSP26 up-regulation resulted from METTL3-mediated translation of m^{6}A-methylated DUSP26 mRNA in a YTHDF1-dependent manner. Notably, DUSP26 silencing reduced aortic valve calcification *in vitro* and *in vivo*. We also identified MDM2 as an E3 ligase ubiquitylating DPP4, while DUSP26 competed with MDM2 for binding to the C-terminus of DPP4, increasing DPP4 protein stability. Moreover, we found that DUSP26 exerted procalcific effects by up-regulating DPP4. These findings pinpoint a previously unidentified regulatory DUSP26-DPP4 axis contributing to CAVD.

Mounting evidence suggests that METTL3-mediated m^{6}A modification plays a crucial role in the pathogenesis of cardiovascular diseases.[35,36] Hence, we demonstrated that METTL3 facilitated the translation of m^{6}A-methylated DUSP26 mRNA through a YTHDF1-dependent pathway, consistent with previous findings.[22,37] We have previously demonstrated that METTL3-mediated m^{6}A modification promotes CAVD progression by regulating TWIST1.[20] In fact, m^{6}A is added to mRNA by a multisubunit writer complex containing METTL3, METTL14, Wilms' tumour-1-associated protein, RNA-binding motif protein 15/15B, Cbl proto-oncogene-like protein 1, and Zinc finger CCCH-type containing 13. There are many types of m^{6}A readers, such as YTHDF1-3, YTH domain-containing proteins, eukaryotic initiation factor 3, and fragile X mental retardation protein.[38] Thus, whether additional m^{6}A writers and readers play distinct roles in the regulation of DUSP26 expression requires further investigation.

Increasing evidence suggests that DUSP26 regulates type 2 diabetes,[9] nonalcoholic fatty liver disease,[8] and chamber-specific growth in the heart.[10] However, its role in CAVD remained uncharacterized. Here, we demonstrated for the first time that DUSP26 was highly expressed in human CAVs and promoted aortic valve calcification *in vitro* and *in vivo*. Patients with severe calcific aortic stenosis develop left ventricular obstruction, which gradually progresses to cardiac hypertrophy and heart failure.[39] In our mouse model, we did not observe any significant changes in the size and function of the heart chamber, possibly because of insufficient hemodynamic stress and the short follow-up period. In a recent study, DUSP26 was found to protect against pressure overload-induced cardiac hypertrophy.[40] This result calls for caution when evaluating the effects of DUSP26 silencing on CAVD-associated cardiac hypertrophy. In our *in vivo* study, we observed variability between the animals and an overlap between groups. This variability may have resulted from various confounding factors, such as interindividual variability for HCD consumption in inbred mice. The mechanisms underlying BAVs and tricuspid aortic valves differ.[41] We used only tricuspid aortic valves and an HCD-fed ApoE$^{-/-}$ mice rather than BAVs and a BAV mouse model; therefore, our results may only be applied to tricuspid CAVD. Whether DUSP26 also plays a role in bicuspid CAVD requires further investigation. DUSP26 has been reported to act as a protein phosphatase.[28] In this study, we demonstrated a novel role of DUSP26, independent of its phosphatase function, in which up-regulated DUSP26 displaces MDM2 from DPP4 in a manner similar to deubiquitination.[42] However, DUSP26 is not a known deubiquitinating enzyme. Thus, this novel function of DUSP26 may provide a new direction for future studies. Moreover, we identified a positive correlation between DUSP26 levels and CAVD severity in CAVD patients; however, the correlation between DUSP26 expression and atherosclerosis severity was not significant. These data may reflect the different pathogenesis between CAVD and atherosclerosis and the specific role of DUSP26 in pro-calcification.

The key role of DPP4 as a crucial modulator in CAVD progression has gained wide acceptance.[14,15,43] However, the feasibility and safety of DPP4 inhibitors for treating CAVD require validation in preclinical and clinical studies. Indeed, saxagliptin, a DPP4 inhibitor, has been proposed to contribute to a higher risk of hospitalization due to heart failure.[16,44] Vildagliptin and linagliptin are associated with an increased risk of bullous pemphigoid.[17] Importantly, the US Food and Drug Administration has warned that DPP4 inhibitors, including sitagliptin, saxagliptin, linagliptin, and alogliptin, may cause severe and persistent arthralgia.[18] Hence, we identified a new endogenous regulatory network independent of DPP4 inhibitors in CAVD in which DUSP26 positively regulated DPP4 by antagonizing the MDM2-mediated DPP4 ubiquitination and degradation. Therefore, our findings provide new mechanistic insights into how DPP4 modulates CAVD progression in an endogenous regulatory manner, which may circumvent the potential adverse effects of DPP4 inhibitors.

Ubiquitination is a crucial posttranslational modification determining protein fate by tagging substrates for proteasomal degradation.[45] E3 ubiquitin ligases, the key enzymes of the ubiquitin-proteasome system, play an important role in pathophysiological processes related to cardiovascular diseases.[46,47] We showed for the first time that MDM2, a key E3 ubiquitin ligase, binds to DPP4, thereby directly catalyzing its ubiquitination and degradation in CAVD. Consistent with these findings, MDM2 promotes the degradation of other proteins, including histone deacetylase 1 protein,[48] TP53,[49] and angiotensin-converting enzyme 2.[50] This is not surprising since ubiquitination is ubiquitous, while E3 ubiquitin ligases are relatively limited. Thus, whether MDM2 ubiquitinates other key regulatory proteins to regulate CAVD progression needs further exploration. Moreover, it has been extensively reported that some substrates, such as Runx2, could be degraded by multiple E3 ubiquitin ligases.[51–53] Hence, further studies are required to investigate whether other E3 ubiquitin ligases target DPP4 for ubiquitin-mediated degradation and hence regulate CAVD progression.

This study has several limitations. First, our microarray-based approach might have introduced selection bias because the initial selection of the potential candidates involved in CAVD was based on a relatively small sample size. Second, the cell-type transcriptome atlas of human aortic valves reveals cell heterogeneity involved in CAVD.[54] Thus, the application of microarray analysis to study the bulk transcriptome could mask the low-abundance changes at the transcriptome level. Third, we did not take into account sex-based differences. To fully address this issue, we should include both males

and females and analyse data separately by sex. Fourth, the enrolment of patients with severe aortic valve calcification in our study might have concealed the factors associated with the development of aortic valve stenosis. There are also limitations of the HCD-fed ApoE$^{-/-}$ mouse model in addition to the extreme hypercholesterolaemia that may not faithfully represent the full progression of human CAVD. The long follow-up of these mice may increase the number of confounding factors (such as sickness, ageing, and even death of mice) affecting the outcome of the *in vivo* findings. At present, there are several commonly used models with obvious advantages; these include NOS3$^{-/-}$/Notch1$^{+/-}$,[55] USP9X$^{fl/Y}$/Cre^{+},[56] and klotho-deficient mice.[57] Further research is required to determine whether DUSP26 inhibition can ameliorate aortic valve calcification in these animal models. In addition, we did not conduct *in vivo* studies using DUSP26 gene-modified mice. Although AAV2-mediated gene silencing is effective for conducting loss-of-function studies, data obtained using DUSP26-knockout mice or a murine model harbouring a cell-type specific deletion of DUSP26 in valve interstitial cells would be more persuasive. Finally, the follow-up duration in our study was relatively short and was insufficient to demonstrate the persistent effect originating from DUSP26 silencing on aortic valve calcification. A longer follow-up study would exclude the events of aortic valve restenosis and verify the long-term effects of DUSP26 silencing on cardiac remodelling.

In conclusion, we showed that DUSP26 was significantly upregulated in CAVD due to enhanced METTL3-mediated translation of m^{6}A-methylated DUSP26 mRNA in a YTHDF1-dependent manner. DUSP26 depletion reduced aortic valve calcification both *in vitro* and *in vivo*. Mechanistically, DUSP26 promoted the osteogenic differentiation of hVICs in aortic valve calcification by stabilizing DPP4. While MDM2 acted as a novel E3 ligase of DPP4, DUSP26 competed with MDM2 for binding to the C-terminus of DPP4 to increase its protein stability in hVICs (*Graphical Abstract*). Therefore, our study provides novel insights into the molecular mechanism regulating DPP4 in the pathogenesis of CAVD and highlights the potential translation of DUSP26-targeted treatment for CAVD in clinical settings.

Supplementary material

Supplementary material is available at *European Heart Journal* online.

Acknowledgments

This work was supported by the National Key Research and Development Program of China (No. 2016YFA0101100, 2016YFA 0100900), the National Natural Science Foundation of China (No. 81974035, 81500300, 91939303, 81820108019), and the Talents Support Program of the China Postdoctoral Science Foundation (BX20200154). We thank Lin Zeng (NewCore BioDataStudio in Shanghai) for sequencing data analysis.

Data availability

All data will be shared upon reasonable request to the corresponding author.

Conflict of interest: none declared.

References

1. Freeman RV, Otto CM. Spectrum of calcific aortic valve disease: pathogenesis, disease progression, and treatment strategies. *Circulation* 2005;**111**:3316–3326.
2. Teo KK, Corsi DJ, Tam JW, Dumesnil JG, Chan KL. Lipid lowering on progression of mild to moderate aortic stenosis: meta-analysis of the randomized placebo-controlled clinical trials on 2344 patients. *Can J Cardiol* 2011;**27**:800–808.
3. Peeters F, Meex SJR, Dweck MR, Aikawa E, Crijns H, Schurgers LJ, Kietselaer B. Calcific aortic valve stenosis: hard disease in the heart: a biomolecular approach towards diagnosis and treatment. *Eur Heart J* 2018;**39**:2618–2624.
4. Jeffrey KL, Camps M, Rommel C, Mackay CR. Targeting dual-specificity phosphatases: manipulating MAP kinase signalling and immune responses. *Nat Rev Drug Discov* 2007;**6**:391–403.
5. Gao L, Zeng H, Zhang T, Mao C, Wang Y, Han Z, Chen K, Zhang J, Fan Y, Gu J, Wang C. MicroRNA-21 deficiency attenuated atherogenesis and decreased macrophage infiltration by targeting Dusp-8. *Atherosclerosis* 2019;**291**:78–86.
6. Kapoor D, Trikha D, Vijayvergiya R, Kaul D, Dhawan V. Conventional therapies fail to target inflammation and immune imbalance in subjects with stable coronary artery disease: a system-based approach. *Atherosclerosis* 2014;**237**:623–631.
7. Kim H, Lee HJ, Oh Y, Choi SG, Hong SH, Kim HJ, Lee SY, Choi JW, Su Hwang D, Kim KS, Kim HJ, Zhang J, Youn HJ, Noh DY, Jung YK. The DUSP26 phosphatase activator adenylate kinase 2 regulates FADD phosphorylation and cell growth. *Nat Commun* 2014;**5**:3351.
8. Ye P, Liu J, Xu W, Liu D, Ding X, Le S, Zhang H, Chen S, Chen M, Xia J. Dual-specificity phosphatase 26 protects against nonalcoholic fatty liver disease in mice through transforming growth factor beta-activated kinase 1 suppression. *Hepatology* 2019;**69**:1946–1964.
9. Gómez-Banoy N, Guseh JS, Li G, Rubio-Navarro A, Chen T, Poirier B, Putzel G, Rosselot C, Pabón MA, Camporez JP, Bhambhani V, Hwang SJ, Yao C, Perry RJ, Mukherjee S, Larson MG, Levy D, Dow LE, Shulman GI, Dephoure N, Garcia-Ocana A, Hao M, Spiegelman BM, Ho JE, Lo JC. Adipsin preserves beta cells in diabetic mice and associates with protection from type 2 diabetes in humans. *Nat Med* 2019;**25**:1739–1747.
10. Yokota T, Li J, Huang J, Xiong Z, Zhang Q, Chan T, Ding Y, Rau C, Sung K, Ren S, Kulkarni R, Hsiai T, Xiao X, Touma M, Minamisawa S, Wang Y. p38 mitogen-activated protein kinase regulates chamber-specific perinatal growth in heart. *J Clin Invest* 2020;**130**:5287–5301.
11. Varin EM, Mulvihill EE, Beaudry JL, Pujadas G, Fuchs S, Tanti JF, Fazio S, Kaur K, Cao X, Baggio LL, Matthews D, Campbell JE, Drucker DJ. Circulating levels of soluble dipeptidyl peptidase-4 are dissociated from inflammation and induced by enzymatic DPP4 inhibition. *Cell Metab* 2019;**29**:320–334. e5.
12. Akoumianakis I, Badi I, Douglas G, Chuaiphichai S, Herdman L, Akawi N, Margaritis M, Antonopoulos AS, Oikonomou EK, Psarros C, Galiatsatos N, Tousoulis D, Kardos A, Sayeed R, Krasopoulos G, Petrou M, Schwahn U, Wohlfart P, Tennagels N, Channon KM, Antoniades C. Insulin-induced vascular redox dysregulation in human atherosclerosis is ameliorated by dipeptidyl peptidase 4 inhibition. *Sci Transl Med* 2020;**12**:eaav8824.
13. Deacon CF. Dipeptidyl peptidase 4 inhibitors in the treatment of type 2 diabetes mellitus. *Nat Rev Endocrinol* 2020;**16**:642–653.
14. Choi B, Lee S, Kim SM, Lee EJ, Lee SR, Kim DH, Jang JY, Kang SW, Lee KU, Chang EJ, Song JK. Dipeptidyl peptidase-4 induces aortic valve calcification by inhibiting insulin-like growth factor-1 signaling in valvular interstitial cells. *Circulation* 2017;**135**:1935–1950.
15. Wang Y, Han D, Zhou T, Zhang J, Liu C, Cao F, Dong N. Melatonin ameliorates aortic valve calcification via the regulation of circular RNA CircRIC3/miR-204-5p/DPP4 signaling in valvular interstitial cells. *J Pineal Res* 2020;**69**:e12666.
16. Scirica BM, Bhatt DL, Braunwald E, Steg PG, Davidson J, Hirshberg B, Ohman P, Frederich R, Wiviott SD, Hoffman EB, Cavender MA, Udell JA, Desai NR, Mosenzon O, McGuire DK, Ray KK, Leiter LA, Raz I; SAVOR-TIMI 53 Steering Committee and Investigators. Saxagliptin and cardiovascular outcomes in patients with type 2 diabetes mellitus. *N Engl J Med* 2013;**369**:1317–1326.
17. Douros A, Rouette J, Yin H, Yu OHY, Filion KB, Azoulay L. Dipeptidyl peptidase 4 inhibitors and the risk of bullous pemphigoid among patients with type 2 diabetes. *Diabetes Care* 2019;**42**:1496–1503.
18. Men P, He N, Song C, Zhai S. Dipeptidyl peptidase-4 inhibitors and risk of arthralgia: a systematic review and meta-analysis. *Diabetes Metab* 2017;**43**:493–500.
19. Yu C, Li L, Xie F, Guo S, Liu F, Dong N, Wang Y. LncRNA TUG1 sponges miR-204-5p to promote osteoblast differentiation through upregulating Runx2 in aortic valve calcification. *Cardiovasc Res* 2018;**114**:168–179.
20. Zhou T, Han D, Liu J, Shi J, Zhu P, Wang Y, Dong N. Factors influencing osteogenic differentiation of human aortic valve interstitial cells. *J Thorac Cardiovasc Surg* 2021;**161**:e163–e185.

21. Wang X, Zhao BS, Roundtree IA, Lu Z, Han D, Ma H, Weng X, Chen K, Shi H, He C. N(6)-methyladenosine modulates messenger RNA translation efficiency. *Cell* 2015;**161**:1388–1399.
22. Shi H, Zhang X, Weng YL, Lu Z, Liu Y, Lu Z, Li J, Hao P, Zhang Y, Zhang F, Wu Y, Delgado JY, Su Y, Patel MJ, Cao X, Shen B, Huang X, Ming GL, Zhuang X, Song H, He C, Zhou T. M. (6)A facilitates hippocampus-dependent learning and memory through YTHDF1. *Nature* 2018;**563**:249–253.
23. Wong FF, Ho ML, Yamagami M, Lam MT, Grande-Allen KJ, Suh J. Effective gene delivery to valvular interstitial cells using adeno-associated virus serotypes 2 and 3. *Tissue Eng Part C Methods* 2015;**21**:808–815.
24. Gössl M, Khosla S, Zhang X, Higano N, Jordan KL, Loeffler D, Enriquez-Sarano M, Lennon RJ, McGregor U, Lerman LO, Lerman A. Role of circulating osteogenic progenitor cells in calcific aortic stenosis. *J Am Coll Cardiol* 2012;**60**:1945–1953.
25. Gošev I, Zeljko M, Đurić Ž, Nikolić I, Gošev M, Ivčević S, Bešić D, Legčević Z, Paić F. Epigenome alterations in aortic valve stenosis and its related left ventricular hypertrophy. *Clin Epigenetics* 2017;**9**:106.
26. Dutta P, Kodigepalli MK, LaHaye S, Thompson JW, Rains S, Nagel C, Thatcher K, Hinton RB, Lincoln J. KPT-330 prevents aortic valve calcification via a novel C/EBPβ signaling pathway. *Circ Res* 2021;**128**:1300–1316.
27. Song R, Fullerton DA, Ao L, Zhao KS, Reece TB, Cleveland JC, Jr., Meng X. Altered microRNA expression is responsible for the pro-osteogenic phenotype of interstitial cells in calcified human aortic valves. *J Am Heart Assoc* 2017;**6**:e005364.
28. Yu W, Imoto I, Inoue J, Onda M, Emi M, Inazawa J. A novel amplification target, DUSP26, promotes anaplastic thyroid cancer cell growth by inhibiting p38 MAPK activity. *Oncogene* 2007;**26**:1178–1187.
29. Ren JX, Cheng Z, Huang YX, Zhao JF, Guo P, Zou ZM, Xie Y. Identification of novel dual-specificity phosphatase 26 inhibitors by a hybrid virtual screening approach based on pharmacophore and molecular docking. *Biomed Pharmacother* 2017;**89**:376–385.
30. Wu W, Jing D, Meng Z, Hu B, Zhong B, Deng X, Jin X, Shao Z. FGD1 promotes tumor progression and regulates tumor immune response in osteosarcoma via inhibiting PTEN activity. *Theranostics* 2020;**10**:2859–2871.
31. Leestemaker Y, Ovaa H. Tools to investigate the ubiquitin proteasome system. *Drug Discov Today Technol* 2017;**26**:25–31.
32. Schlotter F, Halu A, Goto S, Blaser MC, Body SC, Lee LH, Higashi H, DeLaughter DM, Hutcheson JD, Vyas P, Pham T, Rogers MA, Sharma A, Seidman CE, Loscalzo J, Seidman JG, Aikawa M, Singh SA, Aikawa E. Spatiotemporal multi-omics mapping generates a molecular atlas of the aortic valve and reveals networks driving disease. *Circulation* 2018;**138**:377–393.
33. Aikawa E, Libby P. A rock and a hard place: chiseling away at the multiple mechanisms of aortic stenosis. *Circulation* 2017;**135**:1951–1955.
34. Tsimikas S. Potential causality and emerging medical therapies for lipoprotein(a) and its associated oxidized phospholipids in calcific aortic valve stenosis. *Circ Res* 2019;**124**:405–415.
35. Dorn LE, Lasman L, Chen J, Xu X, Hund TJ, Medvedovic M, Hanna JH, van Berlo JH, Accornero F. The N(6)-methyladenosine mRNA methylase METTL3 controls cardiac homeostasis and hypertrophy. *Circulation* 2019;**139**:533–545.
36. Gao XQ, Zhang YH, Liu F, Ponnusamy M, Zhao XM, Zhou LY, Zhai M, Liu CY, Li XM, Wang M, Shan C, Shan PP, Wang Y, Dong YH, Qian LL, Yu T, Ju J, Wang T, Wang K, Chen XZ, Wang YH, Zhang J, Li PF, Wang K. The piRNA CHAPIR regulates cardiac hypertrophy by controlling METTL3-dependent N(6)-methyladenosine methylation of Parp10 mRNA. *Nat Cell Biol* 2020;**22**:1319–1331.
37. Zhang Z, Luo K, Zou Z, Qiu M, Tian J, Sieh L, Shi H, Zou Y, Wang G, Morrison J, Zhu AC, Qiao M, Li Z, Stephens M, He X, He C. Genetic analyses support the contribution of mRNA N(6)-methyladenosine (m(6)A) modification to human disease heritability. *Nat Genet* 2020;**52**:939–949.
38. Zaccara S, Ries RJ, Jaffrey SR. Reading, writing and erasing mRNA methylation. *Nat Rev Mol Cell Biol* 2019;**20**:608–624.
39. Bonow RO, Leon MB, Doshi D, Moat N. Management strategies and future challenges for aortic valve disease. *Lancet* 2016;**387**:1312–1323.
40. Zhao J, Jiang X, Liu J, Ye P, Jiang L, Chen M, Xia J. Dual-specificity phosphatase 26 protects against cardiac hypertrophy through TAK1. *J Am Heart Assoc* 2021;**10**:e014311.
41. Kostina A, Shishkova A, Ignatieva E, Irtyuga O, Bogdanova M, Levchuk K, Golovkin A, Zhiduleva E, Uspenskiy V, Moiseeva O, Faggian G, Vaage J, Kostareva A, Rutkovskiy A, Malashicheva A. Different Notch signaling in cells from calcified bicuspid and tricuspid aortic valves. *J Mol Cell Cardiol* 2018;**114**:211–219.
42. Wan J, Block S, Scribano CM, Thiry R, Esbona K, Audhya A, Weaver BA. Mad1 destabilizes p53 by preventing PML from sequestering MDM2. *Nat Commun* 2019;**10**:1540.
43. Fernández-Ruiz I. Valvular disease: DPP4 inhibitors to prevent aortic valve calcification. *Nat Rev Cardiol* 2017;**14**:190.
44. Seferović PM, Petrie MC, Filippatos GS, Anker SD, Rosano G, Bauersachs J, Paulus WJ, Komajda M, Cosentino F, de Boer RA, Farmakis D, Doehner W, Lambrinou E, Lopatin Y, Piepoli MF, Theodorakis MJ, Wiggers H, Lekakis J, Mebazaa A, Mamas MA, Tschöpe C, Hoes AW, Seferović JP, Logue J, McDonagh T, Riley JP, Milinković I, Polovina M, van Veldhuisen DJ, Lainscak M, Maggioni AP, Ruschitzka F, McMurray JJV. Type 2 diabetes mellitus and heart failure: a position statement from the Heart Failure Association of the European Society of Cardiology. *Eur J Heart Fail* 2018;**20**:853–872.
45. Popovic D, Vucic D, Dikic I. Ubiquitination in disease pathogenesis and treatment. *Nat Med* 2014;**20**:1242–1253.
46. Ji YX, Zhang P, Zhang XJ, Zhao YC, Deng KQ, Jiang X, Wang PX, Huang Z, Li H. The ubiquitin E3 ligase TRAF6 exacerbates pathological cardiac hypertrophy via TAK1-dependent signalling. *Nat Commun* 2016;**7**:11267.
47. Chen H, Moreno-Moral A, Pesce F, Devapragash N, Mancini M, Heng EL, Rotival M, Srivastava PK, Harmston N, Shkura K, Rackham OJL, Yu WP, Sun XM, Tee NGZ, Tan ELS, Barton PJR, Felkin LE, Lara-Pezzi E, Angelini G, Beltrami C, Pravenec M, Schafer S, Bottolo L, Hubner N, Emanueli C, Cook SA, Petretto E. WWP2 regulates pathological cardiac fibrosis by modulating SMAD2 signaling. *Nat Commun* 2019;**10**:3616.
48. Kwon DH, Eom GH, Ko JH, Shin S, Joung H, Choe N, Nam YS, Min HK, Kook T, Yoon S, Kang W, Kim YS, Kim HS, Choi H, Koh JT, Kim N, Ahn Y, Cho HJ, Lee IK, Park DH, Suk K, Seo SB, Wissing ER, Mendrysa SM, Nam KI, Kook H. MDM2 E3 ligase-mediated ubiquitination and degradation of HDAC1 in vascular calcification. *Nat Commun* 2016;**7**:10492.
49. Levine AJ. p53: 800 million years of evolution and 40 years of discovery. *Nat Rev Cancer* 2020;**20**:471–480.
50. Shen H, Zhang J, Wang C, Jain PP, Xiong M, Shi X, Lei Y, Chen S, Yin Q, Thistlethwaite PA, Wang J, Gong K, Yuan ZY, Yuan JX, Shyy JY. MDM2-mediated ubiquitination of angiotensin-converting enzyme 2 contributes to the development of pulmonary arterial hypertension. *Circulation* 2020;**142**:1190–1204.
51. Jones DC, Wein MN, Oukka M, Hofstaetter JG, Glimcher MJ, Glimcher LH. Regulation of adult bone mass by the zinc finger adapter protein Schnurri-3. *Science* 2006;**312**:1223–1227.
52. Shimazu J, Wei J, Karsenty G. Smurf1 inhibits osteoblast differentiation, bone formation, and glucose homeostasis through serine 148. *Cell Rep* 2016;**15**:27–35.
53. Mokuda S, Nakamichi R, Matsuzaki T, Ito Y, Sato T, Miyata K, Inui M, Olmer M, Sugiyama E, Lotz M, Asahara H. Wwp2 maintains cartilage homeostasis through regulation of Adamts5. *Nat Commun* 2019;**10**:2429.
54. Xu K, Xie S, Huang Y, Zhou T, Liu M, Zhu P, Wang C, Shi J, Li F, Sellke FW, Dong N. Cell-type transcriptome atlas of human aortic valves reveal cell heterogeneity and endothelial to mesenchymal transition involved in calcific aortic valve disease. *Arterioscler Thromb Vasc Biol* 2020;**40**:2910–2921.
55. Bosse K, Hans CP, Zhao N, Koenig SN, Huang N, Guggilam A, LaHaye S, Tao G, Lucchesi PA, Lincoln J, Lilly B, Garg V. Endothelial nitric oxide signaling regulates Notch1 in aortic valve disease. *J Mol Cell Cardiol* 2013;**60**:27–35.
56. Majumdar U, Manivannan S, Basu M, Ueyama Y, Blaser MC, Cameron E, McDermott MR, Lincoln J, Cole SE, Wood S, Aikawa E, Lilly B, Garg V. Nitric oxide prevents aortic valve calcification by S-nitrosylation of USP9X to activate NOTCH signaling. *Sci Adv* 2021;**7**:eabe3706.
57. Wirrig EE, Gomez MV, Hinton RB, Yutzey KE. COX2 inhibition reduces aortic valve calcification in vivo. *Arterioscler Thromb Vasc Biol* 2015;**35**:938–947.